

Posterior 180° ^{99m}Tc-Dimercaptosuccinic Acid Renal SPECT

Nan-Jing Peng, C. Gerry Kwok, Yee-Hsuan Chiou, Gang-Hong Jao, Daw-Guey Tsay, Ren-Shyan Liu and H. William Strauss

Departments of Nuclear Medicine and Pediatrics, Veterans General Hospital, Kaohsiung; Department of Nuclear Medicine, Veterans General Hospital, Taipei; National Yang-Ming University, Taiwan, Republic of China; and Division of Nuclear Medicine, Department of Radiology, Stanford University Medical Center, California

As a result of a high percentage of hypoactive upper poles of kidneys in traditional ^{99m}Tc-dimercaptosuccinic acid (DMSA) SPECT, a prospective study was conducted using 180° acquisition technique compared with 360° to minimize tissue attenuation. **Methods:** Anterior 180°, posterior 180° and 360° renal SPECT images were obtained simultaneously using a dual-head camera. Forty-one subjects without renal disease and 16 subjects with 21 cortical defects were included in this study. The total counts of the raw data in the anterior 180°, posterior 180° and full 360° were calculated. Small regions of interest were drawn over the cortex of the kidney on coronal and reoriented sagittal slices. Quantitative evaluation of regional activity was performed on the same frames in all three acquisition methods. **Results:** Comparison of the total renal counts between the anterior and posterior 180° data showed reduced counts in the anterior 180° data collection ($P < 0.01$). Visual evaluation of the reconstructed images from anterior 180°, posterior 180° and full 360° data collection showed the best image uniformity in the posterior 180° image. The upper/lower pole ratio in the posterior 180° renal SPECT images increased significantly in comparison to full 360° renal SPECT images ($P < 0.01$) and anterior 180° SPECT images ($P < 0.01$). The renal defects were more clearly visualized in the posterior 180° renal SPECT images than the full 360° renal SPECT images. The defect/normal cortex ratios in the posterior 180° renal SPECT images were much lower than those from the full 360° SPECT images ($P < 0.01$) and those from the anterior 180° SPECT images ($P < 0.01$). **Conclusion:** The posterior 180° acquisition technique can avoid the problem of hypoactive upper pole and can be less time consuming in ^{99m}Tc-DMSA SPECT images. It also provides superior lesion contrast in the clinical evaluation of patients with renal scarring.

Key Words: kidney; renal scar; SPECT; ^{99m}Tc-dimercaptosuccinic acid.

J Nucl Med 1999; 40:60–63

SPECT with ^{99m}Tc-dimercaptosuccinic acid (DMSA) has been used to detect renal scars. Recent reports suggested higher sensitivity of SPECT compared with planar imaging (1–4) for the detection of focal abnormalities in the kidneys.

However, the kidneys are located posteriorly. In ^{99m}Tc-DMSA renal SPECT images, the signals from the anterior 180° acquisition are remarkably attenuated, which could degrade the quality of a 360° tomogram. The presence of liver and spleen in front of both kidneys also has an attenuation effect on upper poles of kidneys. A high percentage of kidneys with hypoactive upper poles on 360° ^{99m}Tc-DMSA SPECT may be caused by this attenuation problem (5). To determine if 180° SPECT could improve image quality, we conducted a prospective study comparing a posterior 180° with a 360° acquisition technique in patients referred for renal cortical imaging.

MATERIALS AND METHODS

Patients

From October 1, 1996, to April 25, 1997, 134 children with suspicion of urinary tract infection were studied. Patients were evaluated with ^{99m}Tc-DMSA planar and SPECT renal cortical images, renal ultrasonography, urine culture, complete blood count and blood urea nitrogen and creatinine levels. Radionuclide voiding cystoureterograms were performed in 54 patients. All of these examinations were performed within 1 wk of admission to the hospital.

Patients with normal ^{99m}Tc-DMSA planar and SPECT images and normal blood chemistries were placed in group I, and patients with definite cortical defects observed on both planar and SPECT images were placed in group II. In group I, patients with pelvic and calyx distention were excluded by ultrasonography. Forty-one subjects met the criteria for inclusion in group I. The average age was 2 y (range, 2 mo–9 y). Twenty were boys, and 21 were girls. Thirteen of the 41 patients underwent radionuclide voiding cystoureterograms. They all showed negative results. Sixteen patients met the criteria for inclusion in group II. The patients had an average age of 3 y and 4 mo (range, 2 mo–11 y). Eleven were boys, and 5 were girls. Fourteen of the 16 patients underwent radionuclide voiding cystoureterograms, and 9 of them showed vesicoureteral reflux.

Scintigraphic Technique

The ^{99m}Tc-DMSA was prepared from a commercial kit, and the dosage was based on the adult dose of 185 MBq and corrected for the patient's age in years by the following formula:

$$\text{Dose} = (\text{Age} + 1) \times \text{Adult Dose} / (\text{Age} + 7). \quad \text{Eq. 1}$$

The minimum dose was 18.5 MBq.

Received Dec. 26, 1997; revision accepted Apr. 19, 1998.
For correspondence or reprints contact: Ren-Shyan Liu, MD, Department of Nuclear Medicine, Taipei Veterans General Hospital, 201 s. 2, Shih-Pai Road, Taipei, Taiwan, 11217, Republic of China.

Imaging was performed 3 h after injection of the ^{99m}Tc -DMSA. Planar images were recorded on a gamma camera (Siemens orbiter 75; Siemens Corp., Hoffman Estates, IL), with the patient supine, in the posterior, left posterior oblique and right posterior oblique views. Each view was acquired by a total of 300,000 counts in a 256×256 matrix using a low-energy, high-resolution collimator. A 1.25–2.0 zoom was used during acquisition.

SPECT was performed on a digital dual-head camera (Siemens MULTISPECT II) with two low-energy, high-resolution collimators. A series of 64 views was acquired for 40 s each into a 128×128 matrix around a 360° arc with the patient in a supine position. A 1.78 zoom was used. The total acquisition time was 21 min and 20 s. The total counts per study ranged from 1.5 to 4 million counts. Data required to reconstruct the anterior 180° , posterior 180° and 360° renal SPECT images were obtained simultaneously. The raw images were shown in a cinematic format to detect patient motion during and immediately after complete acquisition. Repeat acquisition was performed if patient movement occurred. A software for motion correction (Siemens ICON MPE) was applied if necessary. The total counts of the raw data in the anterior 180° , posterior 180° and 360° were calculated. The data were then processed to produce the 360° and 180° SPECT studies. A butterworth filter and an order of 7 with a cutoff of 0.3 in patients 3 y old and older and 0.4 in patients younger than 3 y old were applied. The same back-projection algorithm and spatial frequency filter were used to reconstruct these three sets of projection data. No attenuation correction was used. Reconstruction was performed with 128×128 matrix centered at the kidneys. The total counts from the largest slice of the anterior 180° , posterior 180° and 360° reconstructed image were calculated.

Small regions of interest (12 pixels) were drawn over the upper and lower poles of the cortex of each kidney on coronal and reoriented sagittal slices for the patients in group I and drawn over the defects and the adjacent normal renal cortex for the patients in group II. Quantitative evaluation of regional activity expressed as mean counts per pixel was performed on the same frames from all three acquisition methods. The maximal upper/lower pole ratio and defects/normal cortex ratio were then calculated.

Statistical Analysis

Statistical analysis was performed using the paired *t* test. Data were expressed as mean \pm SD. A *P* value of <0.05 was considered significant.

RESULTS

A total of 41 patients in group I with 82 apparently healthy kidneys were evaluated with anterior 180° , posterior 180° and full 360° ^{99m}Tc -DMSA SPECT. The organ attenuation was easily observed in the 360° rotating data. A splenic silhouette was observed on 18 of 41 (44%) cases. The total renal counts of the posterior 180° view were significantly greater than those of the anterior 180° view ($P < 0.01$) (Table 1). After data processing, the total counts from the selected slice of the posterior 180° reconstructed image were greater than those from the anterior 180° images, which also were significantly different ($P < 0.05$). Figure 1 shows the SPECT images of normal kidneys reconstructed from the anterior 180° , posterior 180° and 360° acquisition. A more homogeneous ^{99m}Tc -DMSA distribution of both kidneys was observed in the posterior 180° image. The anterior 180°

TABLE 1
Comparison of Total Counts of Raw Data and Reconstructed Image on Three Acquisition Methods in 41 Healthy Subjects

Total counts	Anterior 180°	Posterior 180°
Raw data	$1.34 \times 10^6 \pm 5.7 \times 10^5^*$	$1.43 \times 10^6 \pm 6.9 \times 10^5^*$
Reconstructed image	$1.75 \times 10^5 \pm 7.02 \times 10^4^\dagger$	$1.85 \times 10^5 \pm 7.8 \times 10^4^\dagger$

* $P < 0.01$.
† $P < 0.05$.
Values are expressed as mean \pm SD.

image had the worst uniformity, whereas the 360° image was in-between. The upper-to-lower pole ratio from the posterior 180° renal SPECT images was significantly greater than those from the full 360° renal SPECT images ($P < 0.01$) and the anterior 180° SPECT images ($P < 0.01$) in both the right and left kidney. The results are shown in Table 2.

In group II, 16 patients with 21 cortical defects were evaluated with these three acquisition methods. There were 14 lesions located on the upper pole, 4 on the midzone and 3 on the lower pole. The renal defects were more clearly visualized in the posterior 180° SPECT images than the full 360° SPECT images and were visualized most poorly from the anterior 180° SPECT images (Fig. 2). The defects-to-normal cortex ratio from the posterior 180° renal SPECT images was significantly lower than that from the full 360° SPECT images ($P < 0.01$) and that from the anterior 180° SPECT images ($P < 0.01$), indicating the superior lesion contrast obtained from the posterior 180° technique (Table 3).

DISCUSSION

Several studies have shown that some renal scars can only be detected by renal cortical scintigraphy (6–9). It thus has been recommended that cortical scintigraphy should become the gold standard for the diagnosis of acute pyelonephritis and should be performed routinely in children with acute urinary tract infection (10). Although planar cortical scintigraphy has been used for the detection of renal scarring, recent studies of cortical SPECT suggest enhanced sensitivity for detection of lesions with SPECT (1–4). The sensitivity and specificity of the DMSA scan for the diagnosis of

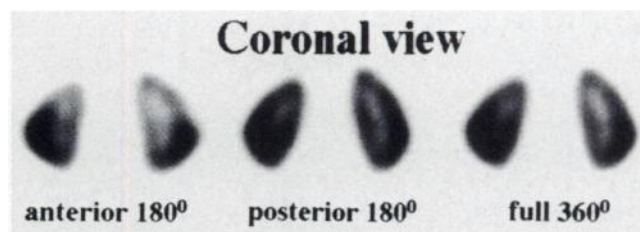


FIGURE 1. Three SPECT images from healthy subject. Posterior 180° SPECT shows best image uniformity (upper to lower pole), whereas anterior 180° shows worst and 360° SPECT in-between image uniformity.

TABLE 2
Comparison of Upper-to-Lower Pole Ratio on Same Frame of Coronal Slice on Three Acquisition Methods in 41 Healthy Subjects

Upper/ lower pole	Anterior 180°	Posterior 180°	Full 360°
Left	0.80 ± 0.12*	0.97 ± 0.13*	0.88 ± 0.11*†
Right	0.83 ± 0.12*	1.02 ± 0.15*	0.93 ± 0.12*†

Values are expressed as mean ± SD.

**P* < 0.01, anterior 180° vs. posterior 180°, anterior 180° vs. full 360° and anterior 180° vs. full 360°.

†*P* < 0.05, left vs. right.

acute pyelonephritis were highly correlated between the scintigraphic and histopathologic finding in an experimentally induced acute pyelonephritis of piglets (11–13). However, a high percentage of kidneys with hypoactive upper poles in ^{99m}Tc-DMSA SPECT was found in many clinics (5). The frequent occurrence of decreased activity in the upper poles on SPECT images, which is not compatible with the finding of planar images, often confuses interpretation of the images. Finding an approach to rectify this problem would make these images easier to evaluate.

Because the kidneys are located posteriorly, more signals are obtained from the posterior 180° collection, whereas more noise is added in the anterior 180°. The anterior images suffer from the effects of attenuation and distance, resulting in lower counts and worse resolution in the region of the kidney than data collected in the posterior arc. In processing ^{99m}Tc-DMSA renal SPECT images, the data from the anterior 180° acquisition make the 360° tomogram exceptionally poor in quality. A posterior 180° data collection procedure, omitting acquisition from the anterior half of the body, was attempted in search of improvement. Although the

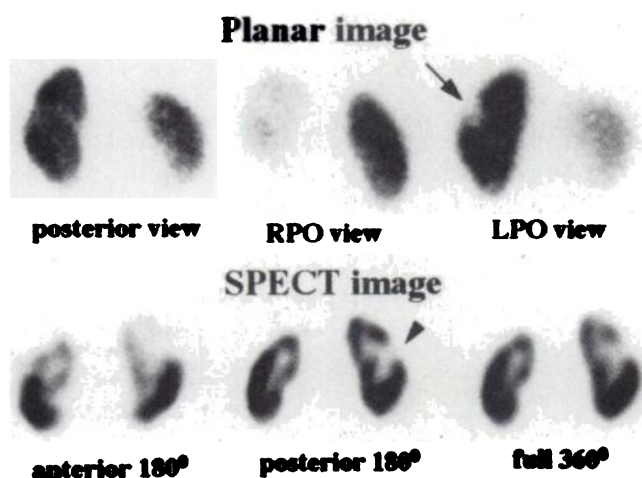


FIGURE 2. DMSA scintigraphy of 9-y-old girl with acute pyelonephritis. High-resolution planar images show cortical defect in midzone of left kidney (arrow). In SPECT images, defect is most clearly visualized in posterior 180° view (arrowhead).

TABLE 3
Defect-to-Normal Renal Cortex Ratio on Same Frame of Coronal Slice on Three Acquisition Methods in 21 Lesions of 16 Patients

	Anterior 180°	Posterior 180°	Full 360°
D:N ratio	0.64 ± 0.16*	0.43 ± 0.13*	0.52 ± 0.13*

**P* < 0.01, anterior 180° vs. posterior 180°, anterior 180° vs. full 360° and posterior 180° vs. full 360°.

Values are expressed as mean ± SD.

D/N ratio = defect-to-normal renal cortex ratio.

liver contributes some activities, especially in the anterior view, our results indicated reduced counts in anterior 180° data collection in comparison to the posterior 180° data collection (*P* < 0.01). Furthermore, the reconstructed SPECT images from the anterior collection also had fewer counts. Thus, the attenuation effects are indeed greater for the images from the anterior 180° acquisition than those from the posterior 180° acquisition.

Sadeleer et al. investigated normal kidneys in 10 young, healthy volunteers with normal clinical history and normal renal ultrasonography using different SPECT modalities and found the presence of hypoactive upper poles in 7 of 20 kidneys, which were observed visually on the coronal slices with up to 35% difference between the upper and lower pole. The mean upper-to-lower pole ratio was 0.79 on the left and 0.87 on the right, respectively (5). In our study, we found 64 hypoactive upper poles (upper pole-to-lower pole ratio of <1) in 82 kidneys with 360° SPECT. The reconstructed images from the anterior 180°, posterior 180° and full 360° data collection showed visible difference in the image uniformity. The upper-to-lower pole ratio was lowest in the anterior 180° image and highest in the posterior 180° image. The 360° image showed the ratios in-between. There is a 20% reduction in the upper pole on the left and a 17% reduction on the right from the anterior 180° image. For the 360° technique, there is a 12% reduction in the upper pole on the left and a 7% on the right. However, in the posterior 180° image, the data are very close to 1. The posterior 180° technique gives more uniform upper to lower pole image. Therefore, the hypoactive upper pole caused by the attenuation effect can be avoided. It is possible to eliminate false-positive defects in the upper pole using the posterior technique. Sadeleer et al. also found that hypoactive upper poles are mainly on the left, but they had no clear explanation for this observation. Identical findings occurred in our cases. Splenic attenuation, visually observed in the 360° rotating data in 18 of 41 patients, is a likely explanation for this finding in the left kidney. The mean upper-to-lower pole ratio was lower for the left kidney than for the right kidney. We agree that splenic impression should be excluded in the diagnosis criteria of renal scarring (2,3,14).

The posterior 180° acquisition method, using the data from only a 180° sweep as opposed to the 360° data

collection, used only half the acquired data but provided more uniform-appearing kidneys and higher lesion contrast. When a single-detector gamma camera is used to acquire the data, acquisition time could be shortened. However, even when multidetector instruments are used, reconstructing the data from the posterior perspective only resulted in more effective renal uptake. Because the major goal of this study was to evaluate the superiority of the posterior acquisition of DMSA SPECT in comparison to 360° acquisition, the results of this study do not necessarily indicate that posterior acquisition improves overall sensitivity and specificity of DMSA SPECT. Further studies will be conducted to verify this issue.

CONCLUSION

The spatial distribution of kidneys in the body allows a reasonable use of a 180° sweep. The posterior 180° acquisition technique can provide more useful information than the 360° technique. The commonly observed hypoactive upper pole, which is probably caused by attenuation from the spleen and liver, could be avoided by the posterior 180° technique. The posterior 180° acquisition method provides the advantage of better lesion contrast and shorter acquisition time. We conclude that the posterior 180° acquisition technique can give more accurate information and can be less time consuming.

ACKNOWLEDGMENTS

We thank Ger Luo-Ping, MPH, for statistical assistance. This work was supported by grant NSC 87-2314-B-075B-001 from the National Science Council, Taiwan, Republic of China. This study was presented at the 44th annual meeting of the Society of Nuclear Medicine, San Antonio, Texas, June 1-5, 1997.

REFERENCES

1. Yen TC, Chen WP, Chang SL, et al. Technetium-99m DMSA renal SPECT in diagnosing and monitoring pediatric acute pyelonephritis. *J Nucl Med.* 1996;37:1349-1353.
2. Mastin ST, Drane WE, Irvani A. Tc-99m DMSA SPECT imaging in patients with acute symptoms or history of UTI. Comparison with ultrasonography. *Clin Nucl Med.* 1995;20:407-412.
3. Mouratidis B, Ash JM, Gilday DL. Comparison of planar and SPECT Tc-99m DMSA scintigraphy for the detection of renal cortical defects in children. *Nucl Med Commun.* 1993;14:82-86.
4. Takeda M, Katayama Y, Tsutsui T, et al. Value of dimercaptosuccinic acid single photon emission computed tomography and magnetic resonance imaging in detecting renal injury in pediatric patients with vesicoureteral reflux. *Eur Urol.* 1994;25:320-325.
5. Sadeleer CDe, Bossuyt A, Goes E, Piepsz A. Renal technetium-99m DMSA SPECT in normal volunteers. *J Nucl Med.* 1996;37:1346-1349.
6. Sreenarasimhalah V, Alon US. Uroradiologic evaluation of children with urinary tract infection: are both ultrasonography and renal cortical scintigraphy necessary? *J Pediatr.* 1995;127:373-377.
7. Jakobsson B, Nolstedt L, Svensson L, Soderlundh S, Berg U. Technetium-99m dimercaptosuccinic acid scan in the diagnosis of acute pyelonephritis in children: relation to clinical and radiological findings. *Pediatr Nephrol.* 1992;6:328-334.
8. Rushton HG, Majd M, Jantusch B, Wiedermann L, Belman AB. Renal scarring following reflux and nonreflux pyelonephritis in children: evaluation with technetium-99m dimercaptosuccinic acid scintigraphy. *J Urol.* 1992;147:1327-1332.
9. Verber IG, Meller ST. Serial Tc-99m dimercaptosuccinic acid (DMSA) scans after urinary infections presenting before the age of 5 years. *Arch Dis Child.* 1989;64:1533-1537.
10. Andrich MP, Majd M. Diagnostic imaging in the evaluation of the first urinary tract infection in infants and young children. *Pediatrics.* 1992;90:436-441.
11. Giblin JG, O'Connor KP, Fildes RD, et al. The diagnosis of acute pyelonephritis in the piglet using single-photon emission computerized tomography dimercaptosuccinic acid scintigraphy: a pathological correlation. *J Urol.* 1993;150:759-762.
12. Majd M, Rushton HG, Chandra R, Andrich MP, Tardif CP, Rashti F. Technetium-99m DMSA renal cortical scintigraphy to detect experimental acute pyelonephritis in piglets: comparison of planar (pinhole) and SPECT imaging. *J Nucl Med.* 1996;37:1731-1734.
13. Rushton HG, Majd M, Chandra R, et al. Evaluation of Tc-99m dimercaptosuccinic acid renal scans in experimental acute pyelonephritis in piglets. *J Urol.* 1988;140:1169-1174.
14. Farnsworth RH, Rosshigh MA, Leighton DM, et al. The detection of reflux nephropathy in infants by Tc-99m dimercaptosuccinic acid studies. *J Urol.* 1991;145:542-546.